INTERNATIONAL JOURNAL FOR NUMERICAL METHODS IN FLUIDS
Int. J. Numer. Meth. Fluids **29**: 535–554 (1999)

A CONSERVATIVE STABILIZED FINITE ELEMENT METHOD FOR THE MAGNETO-HYDRODYNAMIC EQUATIONS

NIZAR BEN SALAH[a,b], AZZEDDINE SOULAIMANI[b], WAGDI G. HABASHI[a,*] AND MICHEL FORTIN[c]

[a] *CFD Laboratory, ER-301, Department of Mechanical Engineering, Concordia University, 1455 de Maisonneuve Blvd. W., Montreal, Quebec H3G 1M8, Canada*
[b] *Ecole de technologie supérieure, Département de génie mécanique, Université du Québec, 1100 rue Notre-Dame Ouest, Montreal, Quebec H3C 1K3, Canada*
[c] *Département de mathématiques et de statistique, Université Laval, Ste-Foy, Quebec G1K 7P4, Canada*

SUMMARY

This work presents a finite element solution of the 3D magneto-hydrodynamics equations. The formulation takes explicitly into account the local conservation of the magnetic field, giving rise to a conservative formulation and introducing a new scalar variable. A stabilization technique is used in order to allow equal linear interpolation on tetrahedral elements of all the variables. Numerical tests are performed in order to assess the stability and the accuracy of the resulting methods. The convergence rates are calculated for different stabilization parameters. Well-known MHD benchmark tests are calculated. Results show good agreement with analytical solutions. Copyright © 1999 John Wiley & Sons, Ltd.

KEY WORDS: finite element method; MHD equations; conservative formulation; stabilization techniques; Hartmann flow; MHD Rayleigh flow; numerical solutions

1. INTRODUCTION

Numerical methods for magneto-hydrodynamic (MHD) equations have attracted the interest of many researchers over the past two decades. The literature presents mainly two trends for formulating MHD problems: using the magnetic field **B** as the independent variable or using the vector potential **A** with the associated scalar potential. Choosing between the two formulations depends on many factors and, especially on the physical problem to be solved. The methods of solving for the vector potential are well-known in the pure electromagnetic context [1–4]. One can consult Biro and Preis [5] for a general overview of the vector potential methods, and some of their electromagnetic applications.

In the context of MHD, these methods have also been popular and intensively used to solve MHD equations in different situations. Fautrelle [6] used a vector potential formulation in solving the magnetic part of electromagnetic stirring problems. He treated it as a pure electromagnetic problem by dropping motion effects in the Maxwell equations. Mestel [7] examined, both analytically and numerically, the process of levitation melting of metals.

* Correspondence to: CFD Laboratory, Department of Mechanical Engineering, Concordia University, 1455 de Maisonneuve Blvd. W., ER-301, Montreal, Quebec H3G 1M8, Canada.

CCC 0271–2091/99/050535–20$17.50

Received July 1997
Revised October 1997

Lympany *et al.* [8] presented numerical results for the MHD effects in aluminium reduction cells. Assuming a steady two-dimensional phenomenon, they solved for the scalar potential ϕ and deduced the magnetic field using the Biot–Savart law. Besson *et al.* [9] developed a two-dimensional finite element method for solving both the MHD and the free-surface problems associated with electromagnetic casting (EMC). They represented the outside potential by an integral equation, so their method could be described as a FEM/BEM one. More recently, Conraths [10] described the magnetic field by an electric vector potential and a magnetic scalar potential, for modeling an inductive heating device for thin moving metal strips. While this literature survey is by no means exhaustive, it illustrates the general use of vector potential formulations, indicates their popularity and wide use in the literature and underlines the main idea of these formulations: namely, that the introduction of the vector potential circumvents the explicit imposition of the magnetic free-divergence constraint since the conservation of the magnetic field is implicitly respected within the definition of the vector potential.

The second main trend in the literature consists in solving directly for the magnetic field **B**. Doing so would normally result in an overdetermined system of equations. This can be overcome by dropping the free-divergence equation and the terms implying this same divergence within the magnetic induction equation. The resulting vectorial equation is a diffusion–convection 'Helmholtz'-like equation. Such a formulation has also been thoroughly used for the solution of MHD equations. One can consult Sazhin *et al.* [11], where the authors solved the resulting Helmholtz equation with a finite difference method, or Gardner and Gardner [12], who presented a two-dimensional bi-cubic B-spline finite element method for the MHD channel flow. Once again, while this literature survey of the 'Helmholtz' formulation is not meant to be either exhaustive or complete, it indicates that these formulations have already been used by many authors and in many different contexts.

These two main families of formulations share a feature in common. Both do not explicitly impose the free-divergence condition on the magnetic field. To the best of the authors knowledge, only Oki and Tanahashi [13,14] have developed numerical schemes that explicitly satisfy the solenoidal condition of the magnetic field. They introduced a variable called hydromagnetic cross-helicity $G = \mathbf{u} \cdot \mathbf{B}$ and retained the free-divergence equation within their system of equations. They presented results for the natural convection of a thermoelectrically conducting fluid under a magnetic field. The actual work, initiated in [15], aimed at developing a conservative finite element method for the MHD equations. 'Conservation' means an appropriate satisfaction of the free-divergence condition by the numerical scheme. Therefore, in this paper a conservative and stable finite element solution of the 3D MHD equations is presented, with a method that takes into account both the magnetic induction and the magnetic field conservation equations.

The remainder of the paper is organized in five sections. In the first section, the MHD governing equations are presented and reviewed. The above cited Helmholtz and vector potential formulations are presented and briefly commented upon. In the second section, the conservative method is developed. It will be shown that the introduction of a Lagrange multiplier within the system of equations circumvents the overdetermination of the system, while giving rise to equivalent equations if appropriate boundary conditions are prescribed. In the third section, the Galerkin weak form of the equations is obtained, giving rise to a mixed finite element formulation. A stabilization technique is introduced to circumvent the usual Brezzi–Babuska stability conditions and to allow equal interpolation for all the variables. It is also seen that a penalty factor is introduced in order to force the magnetic divergence towards zero. In the fourth section, systematic numerical experiments are carried out to assess the

accuracy and stability of the different methods resulting from our formulation. Tests are then run to validate the numerical code that has been developed. The main conclusions are summarized in the last section.

2. THE GOVERNING EQUATIONS

The MHD equations can be derived from the Maxwell equations, Ohm's law for a moving medium and the principle of conservation of the electric charge (Landau *et al.* [16]). Under the classical assumptions of neglecting both the displacement current $\partial \mathbf{D}/\partial t$ and the time variation of the charge density $\partial q/\partial t$, when compared with the electric current density $\mathbf{j}$ ($\mathbf{D}$ and q are the electric induction field and the electric charge density respectively), assuming the permittivity ϵ, the magnetic permeability μ and the electric conductivity σ to be constants (ϵ and μ are equal to those of free space), one can write:

$$\nabla \times \mathbf{B} = \mu \mathbf{j}, \tag{1}$$

$$\nabla \times \mathbf{E} = -\frac{\partial \mathbf{B}}{\partial t}, \tag{2}$$

$$\nabla \cdot \mathbf{B} = 0, \tag{3}$$

$$\mathbf{j} = \sigma(\mathbf{E} + \mathbf{U} \times \mathbf{B}), \tag{4}$$

$$\nabla \cdot \mathbf{j} = 0, \tag{5}$$

where $\mathbf{B}$ and $\mathbf{E}$ are respectively, the magnetic and electric fields. Noting that by virtue of (1) the divergence of the electric current density $\mathbf{j}$ is zero, Equation (5) becomes superfluous. Taking the curl of Ohm's law (4), term by term, and making use of Faraday's and Ampere's laws (1) and (2), one obtains:

$$\frac{\partial \mathbf{B}}{\partial t} - \nabla \times (\mathbf{U} \times \mathbf{B}) + \eta \nabla \times (\nabla \times \mathbf{B}) = 0, \tag{6}$$

where $\eta = 1/\mu\sigma$, is the magnetic diffusivity coefficient. Once Equation (6) is solved for the magnetic field $\mathbf{B}$, the electric field can be deduced from the following equation:

$$\mathbf{E} = \frac{\nabla \times \mathbf{B}}{\eta} - \mathbf{U} \times \mathbf{B} \tag{7}$$

and then the electric current density $\mathbf{j}$ can be calculated from Equation (4).

Equation (6) is the best known and used form of the magnetic induction equation. It consists of a diffusive second-order curl–curl term, a convective first-order curl term and a hyperbolic in time first-order term. It brings the advantage of directly relating the main hydrodynamic quantity, namely the velocity field, to the main electromagnetic one, namely the magnetic field, without any interference. Here it should be pointed out, that the magnetic free-divergence constraint (3), which was not used, is implicit in Equation (6). Indeed, if the divergence of Equation (6) is taken, term by term, one obtains the following condition on the divergence of $\mathbf{B}$:

$$\frac{\partial(\nabla \cdot \mathbf{B})}{\partial t} = 0. \tag{8}$$

Equation (8) stipulates that the divergence of **B** remains constant over time and thus zero if it is initially null. However, it is well-known that in general, the construction of such an initial divergence-free field is not an easy task. Thus, the resulting system of MHD equations consists of both Equations (3) and (6).

2.1. The 'Helmholtz' formulation

Using the vector identity stating that:

$$\nabla \times (\nabla \times \mathbf{B}) = -\nabla^2 \mathbf{B} + \nabla(\nabla \cdot \mathbf{B}), \tag{9}$$

the magnetic induction equation (6) could be rewritten as:

$$\frac{\partial \mathbf{B}}{\partial t} - \nabla \times (\mathbf{U} \times \mathbf{B}) - \eta \nabla^2 \mathbf{B} + \eta \nabla(\nabla \cdot \mathbf{B}) = 0. \tag{10}$$

One can make use of Equation (3) in order to obtain the following 'Helmholtz' equation:

$$\frac{\partial \mathbf{B}}{\partial t} - \nabla \times (\mathbf{U} \times \mathbf{B}) - \eta \nabla^2 \mathbf{B} = 0 \tag{11}$$

and hence reducing the MHD system of Equations (3) and (6) to Equation (11) with the appropriate set of boundary conditions. As stated in Section 1, many numerical methods for MHD problems have been based on this formulation. It should be noted that circumventing the constraint (3) by solving Equation (11) results in a much simpler system to solve. However, Equation (11) does not state anymore that the divergence of **B** remains constant over time. It only states that:

$$\frac{\partial(\nabla \cdot \mathbf{B})}{\partial t} = \nabla \cdot (\eta \nabla^2 \mathbf{B}). \tag{12}$$

One can expect this divergence to play a non-negligible role in the discrete form of the weak problem associated with the continuous strong problem (11).

Remark 1:

The authors would like to point out here an analogy with the Stokes problem for an incompressible fluid with constant viscosity. The Stokes problem is written as:

$$-\nabla \cdot (2\eta\gamma(\mathbf{U})) + \nabla p = \mathbf{F}, \tag{13}$$

$$\nabla \cdot \mathbf{U} = 0, \tag{14}$$

with η, in this case being the dynamic viscosity coefficient and $\gamma(\mathbf{U})$ being the symmetric part of the velocity gradient tensor. If from (13) and (14) one derives the equations for the special case of constant viscosity η, then by making use of Equation (14), one gets:

$$-\eta \nabla^2 \mathbf{U} + \nabla p = \mathbf{F}. \tag{15}$$

Although Equation (14) has been used in order to derive (15), it is well-known in the context of the fluid dynamics, that one has to keep the divergence-free constraint (14) within the system of equations, while developing any numerical solution of the Stokes problem. The pressure p plays the role of a Lagrange multiplier in order to enforce the velocity divergence-free condition. This analogy is also valid for the Navier–Stokes equations. The magnetic continuity equation (3) is the electromagnetic equivalent of the hydrodynamic continuity equation (14) and deserves considerable attention.

2.2. The vector potential formulation

Alternative to the above derivation of equations, one can start from Ohm's law (4), make use of Equation (1), and noting that by definition:

$$\mathbf{E} = -\nabla\phi - \frac{\partial \mathbf{A}}{\partial t}, \tag{16}$$

write the following equation in terms of the vector potential $\mathbf{A}$:

$$\frac{\partial \mathbf{A}}{\partial t} - \mathbf{U} \times (\nabla \times \mathbf{A}) + \eta \nabla \times (\nabla \times \mathbf{A}) + \nabla\phi = 0, \tag{17}$$

the vector potential $\mathbf{A}$ being defined as:

$$\mathbf{B} = \nabla \times \mathbf{A}. \tag{18}$$

Introducing such a vector brings the advantage of implicitly respecting the divergence-free constraint (3). However, this technique of introducing the vector potential presents a challenging problem when gauging the field $\mathbf{A}$ and dealing with its boundary conditions in order to enforce the uniqueness of the solution of the magnetic field.

3. THE CONSERVATIVE FORMULATION

In order to introduce this family of formulations, let us recall the 'Helmholtz' formulation. The idea leading to this formulation is that the system composed of Equations (3) and (6) is overspecified and leads to more equations than unknowns. For example, in the three-dimensional case and if the velocity field is assumed known, the system of equations composed by Equations (3) and (6), gives rise to four linear equations with three unknowns. In Jiang *et al.* [17], the authors showed that an equivalent situation exists in the pure electromagnetic context. They demonstrated that the first-order div–curl Maxwell's system of equations (1)–(3) is not an overdetermined one. They showed that by introducing two dummy scalar variables, they end up with an equivalent system of eight equations with eight unknowns. They underlined the dangers of circumventing the 'overspecification' of system (1)–(3) by dropping the free-divergence equation (3). These dangers are related to the ellipticity of the system, the uniqueness of the solution and the ensuing spurious numerical solutions that may appear.

Using the same technique, it will be shown that the second-order system of Equations (3) and (6) is not an overspecified one.

Let Ω be a bounded, simply connected, convex and open domain, which is included in $\mathbf{R}^3$, with a piecewise smooth boundary Γ, the union of Γ_1 and Γ_2, with $\mathbf{n}$, the unity normal outward vector. Let Equations (3) and (6) hold in the domain Ω and be associated with appropriate boundary conditions on Γ. Adding the gradient of a scalar variable to Equation (6), one gets the following new equation:

$$\frac{\partial \mathbf{B}}{\partial t} - \nabla \times (\mathbf{U} \times \mathbf{B}) + \eta \nabla \times (\nabla \times \mathbf{B}) + \nabla p = 0 \quad \text{in } \Omega. \tag{19}$$

Let the homogeneous Dirichlet condition

$$p = 0 \tag{20}$$

hold on the boundary Γ. Taking the divergence of Equation (19) and using Equation (3), one gets:

$$\Delta p = 0 \quad \text{in } \Omega. \tag{21}$$

As Equation (21) is submitted to the boundary condition (20), this leads to the unique physical solution $p = 0$ over all the domain Ω. Thus, the scalar p is really a dummy variable (which in theory should be null) and the system of Equations (3) and (19) is equivalent to the system (3) and (6). The new system of equations has in the three-dimensional case, four equations with four unknowns and is no longer overdetermined. By analogy to the Stokes and the Navier–Stokes equations, p is interpreted as a Lagrange multiplier used to enforce the divergence-free condition (3).

Remark 2:

Equation (19) could be rewritten in many equivalent forms. Particularly, after making use of the vector identity (9), one gets the following equivalent equation:

$$\frac{\partial \mathbf{B}}{\partial t} - \nabla \times (\mathbf{U} \times \mathbf{B}) - \eta \nabla^2 \mathbf{B} + \eta \nabla(\nabla \cdot \mathbf{B}) + \nabla p = 0 \quad \text{in } \Omega. \tag{22}$$

In the rest of the present work, Equation (22) along with the constraint (3), is used as the model for the MHD equations.

Remark 3:

It is easily predictable that non-respect of the constraint (3) leads to inaccurate numerical solutions. In order to show this, suppose one discards the divergence-free equation and retains only Equation (10). Let for simplicity, the velocity field be equal to zero, and assume the problem to be steady. From (10), one obtains:

$$\nabla \times (\nabla \times \mathbf{B}) = 0 \quad \text{in } \Omega, \tag{23}$$

with the most probable boundary conditions

$$\mathbf{n} \cdot \mathbf{B} = 0 \quad \text{on } \Gamma_1, \tag{24}$$

$$\mathbf{n} \times \mathbf{B} = 0 \quad \text{on } \Gamma_2. \tag{25}$$

The solution of Equation (23) subject to the boundary conditions (24) and (25) is not unique. It admits a kernel composed of the gradient of scalar variables satisfying the conditions (24) and (25). Any numerical method for problem (23)–(25) will fail to provide a unique solution. The constraint (3) should thus be taken into account and it behaves like a gauge condition filtering the divergence-free solution. The respect of this condition reduces the kernel of spurious solutions to a unique null scalar function.

Indeed, according to the unity partition theorem (Brezis [18]), there exist scalar functions ϕ that are C^∞, satisfying $\partial\phi/\partial n = 0$ on Γ_1, $\mathbf{n} \times \nabla\phi = 0$ on Γ_2 and $\phi = 0$ in a part of Ω. Thus, if $\mathbf{B}_0$ is a particular solution of (23)–(25), then any vector $\mathbf{B} = \mathbf{B}_0 + \nabla\phi$ is also a solution. But if the vector solution has to satisfy the divergence-free condition, then $\Delta\phi = 0$ in Ω. As $\partial\phi/\partial n = 0$ on Γ_1 and $\mathbf{n} \times \nabla\phi = 0$ on Γ_2, then ϕ is equal to a constant in Ω. Since ϕ is prescribed zero in a part of the domain, then $\phi = 0$ over all the domain Ω.

4. VARIATIONAL FORMULATION AND DISCRETIZATION

4.1. The Galerkin method

The Galerkin weighted residual formulation for the system of Equations (3) and (19) is obtained through multiplying the two equations by two test functions $\mathbf{B}^*$ and p^* respectively, chosen in two appropriate functional spaces. After integrating the resulting equations over the whole domain Ω, one gets:

$$\int_\Omega \mathbf{B}^* \cdot \left(\frac{\partial \mathbf{B}}{\partial t}\right) \mathrm{d}\Omega - \eta \int_\Omega \mathbf{B}^* \cdot \nabla^2 \mathbf{B} \, \mathrm{d}\Omega + \eta \int_\Omega \mathbf{B}^* \cdot \nabla(\nabla \cdot \mathbf{B}) \, \mathrm{d}\Omega - \int_\Omega \mathbf{B}^* \cdot \nabla \times (\mathbf{U} \times \mathbf{B}) \, \mathrm{d}\Omega + \int_\Omega \mathbf{B}^* \cdot \nabla p \, \mathrm{d}\Omega = 0, \tag{26}$$

$$\int_\Omega p^* (\nabla \cdot \mathbf{B}) \, \mathrm{d}\Omega = 0, \tag{27}$$

for all $\mathbf{B}^*$ and all p^*.

Applying the divergence theorem, the weak form of the Galerkin formulation is obtained as:

$$\int_\Omega \mathbf{B}^* \cdot \left(\frac{\partial \mathbf{B}}{\partial t}\right) \mathrm{d}\Omega + \eta \int_\Omega \nabla \mathbf{B}^* \cdot \nabla \mathbf{B} \, \mathrm{d}\Omega - \int_\Omega \mathbf{B}^* \cdot \nabla \times (\mathbf{U} \times \mathbf{B}) \, \mathrm{d}\Omega + \int_\Omega \mathbf{B}^* \cdot \nabla p \, \mathrm{d}\Omega - \eta \int_\Omega (\nabla \cdot \mathbf{B})(\nabla \cdot \mathbf{B}^*) \, \mathrm{d}\Omega - \eta \int_\Gamma (\mathbf{n} \cdot \nabla \mathbf{B}^*) \cdot \mathbf{B}^* \, \mathrm{d}\Gamma + \eta \int_\Gamma (\mathbf{n} \cdot \mathbf{B}^*)(\nabla \cdot \mathbf{B}) \, \mathrm{d}\Gamma = 0, \tag{28}$$

$$\int_\Omega p^* (\nabla \cdot \mathbf{B}) \, \mathrm{d}\Omega = 0. \tag{29}$$

In the usual manner, the discrete problem associated with the weak form (28) and (29) can be established as:

$$\int_\Omega \mathbf{B}_h^* \cdot \left(\frac{\partial \mathbf{B}}{\partial t}\right) \mathrm{d}\Omega + \eta \int_\Omega \nabla \mathbf{B}_h^* \cdot \nabla \mathbf{B}_h \, \mathrm{d}\Omega - \int_\Omega \mathbf{B}_h^* \cdot \nabla \times (\mathbf{U} \times \mathbf{B}_h) \, \mathrm{d}\Omega + \int_\Omega \mathbf{B}_h^* \cdot \nabla p_h \, \mathrm{d}\Omega - \eta \int_\Omega (\nabla \cdot \mathbf{B}_h)(\nabla \cdot \mathbf{B}_h^*) \, \mathrm{d}\Omega - \eta \int_\Gamma (\mathbf{n} \cdot \nabla \mathbf{B}_h) \cdot \mathbf{B}_h^* \, \mathrm{d}\Gamma + \eta \int_\Gamma (\mathbf{n} \cdot \mathbf{B}_h^*)(\nabla \cdot \mathbf{B}_h) \, \mathrm{d}\Gamma = 0, \tag{30}$$

$$\int_\Omega p_h^* (\nabla \cdot \mathbf{B}_h) \, \mathrm{d}\Omega = 0, \tag{31}$$

for all $\mathbf{B}_h^*$ and p_h^* belonging to some finite-dimensional functional subspaces.

The variational problem formulated by Equations (30) and (31) is of mixed type and presents many similarities with the mixed variational formulation for the Navier–Stokes equations (Brezzi and Fortin [19]). Hence, it requires the respect of the inf–sup stability condition, also called the L.B.B. condition in order to find a stable numerical solution ($\mathbf{B}_h^*$, p_h^*). In practice, the respect of this stability condition implies the use of different approximations for the two variables ($\mathbf{B}_h^*$, p_h^*). In three dimensions, elements respecting the L.B.B. condition could prove expensive with regard to execution time and memory storage. Moreover, the implementation of three dimensions mixed formulations is quite complicated. Another way of obtaining a stable finite element method for the system (30) and (31) is by circumventing the L.B.B. condition (Hughes *et al.* [20]).

4.2. The stabilized finite element method

Suppose $\Omega_h = \cup \Omega_e$, a certain partition of the domain Ω into elements and h the 'size' of an element Ω_e. Following Brezzi and Pitkaranta [21], the continuity equation (31) is modified as:

$$\int_\Omega p_h^*(\nabla \cdot \mathbf{B}_h)\,\mathrm{d}\Omega + \sum_{\Omega_e \in \Omega_h} \tau_1 \int_{\Omega_e} \nabla p_h \cdot \nabla p_h^*\,\mathrm{d}\Omega = 0, \tag{32}$$

where τ_1 is a function of the mesh size h to be specified.

This stabilization technique is equivalent to augmenting the continuity equation (3) of the strong problem with a Laplacian dissipation term of the scalar p and has already been used successfully for the Navier–Stokes incompressible and compressible flows (Baruzzi *et al.* [22]). Hence, the stabilized formulation can be introduced as:

$$\int_\Omega \mathbf{B}_h^* \cdot \left(\frac{\partial \mathbf{B}}{\partial t}\right) \mathrm{d}\Omega + \eta \int_\Omega \nabla \mathbf{B}_h^* \cdot \nabla \mathbf{B}_h\,\mathrm{d}\Omega - \int_\Omega \mathbf{B}_h^* \cdot \nabla \times (\mathbf{U} \times \mathbf{B}_h)\,\mathrm{d}\Omega + \int_\Omega \mathbf{B}_h^* \cdot \nabla p_h\,\mathrm{d}\Omega$$
$$- \eta \int_\Omega (\nabla \cdot \mathbf{B}_h)(\nabla \cdot \mathbf{B}_h^*)\,\mathrm{d}\Omega - \eta \int_\Gamma (\mathbf{n} \cdot \nabla \mathbf{B}_h) \cdot \mathbf{B}_h^*\,\mathrm{d}\Gamma + \eta \int_\Gamma (\mathbf{n} \cdot \mathbf{B}_h^*)(\nabla \cdot \mathbf{B}_h)\,\mathrm{d}\Gamma = 0, \tag{33}$$

$$\int_\Omega p_h^*(\nabla \cdot \mathbf{B}_h)\,\mathrm{d}\Omega + \sum_{\Omega_e \in \Omega_h} \tau_1 \int_{\Omega_e} \nabla p_h \cdot \nabla p_h^*\,\mathrm{d}\Omega = 0. \tag{34}$$

Once the stability of the formulation is insured, the volume integral emanating from the $\nabla(\nabla \cdot \mathbf{B})$ term is penalized with a term τ_2 in order to enforce the magnetic divergence toward small values when the convection is dominant (i.e. small values of η). Then, the implemented formulation could be presented as:

$$\int_\Omega \mathbf{B}_h^* \cdot \left(\frac{\partial \mathbf{B}}{\partial t}\right) \mathrm{d}\Omega + \eta \int_\Omega \nabla \mathbf{B}_h^* \cdot \nabla \mathbf{B}_h\,\mathrm{d}\Omega - \int_\Omega \mathbf{B}_h^* \cdot \nabla \times (\mathbf{U} \times \mathbf{B}_h)\,\mathrm{d}\Omega + \int_\Omega \mathbf{B}_h^* \cdot \nabla p_h\,\mathrm{d}\Omega$$
$$+ (\tau_2 - \eta) \int_\Omega (\nabla \cdot \mathbf{B}_h)(\nabla \cdot \mathbf{B}_h^*)\,\mathrm{d}\Omega - \eta \int_\Gamma (\mathbf{n} \cdot \nabla \mathbf{B}_h) \cdot \mathbf{B}_h^*\,\mathrm{d}\Gamma + \eta \int_\Gamma (\mathbf{n} \cdot \mathbf{B}_h^*)(\nabla \cdot \mathbf{B}_h)\,\mathrm{d}\Gamma = 0, \tag{35}$$

$$\int_\Omega p_h^*(\nabla \cdot \mathbf{B}_h)\,\mathrm{d}\Omega + \sum_{\Omega_e \in \Omega_h} \tau_1 \int_{\Omega_e} \nabla p_h \cdot \nabla p_h^*\,\mathrm{d}\Omega = 0. \tag{36}$$

The stabilized method defined by (35) and (36) allows the use of equal interpolation for the two variables ($\mathbf{B}_h^*$, p_h^*), thus facilitating the implementation and permitting the use of cheaper elements. In this work, all the variables are interpolated by linear functions on tetrahedral elements.

5. NUMERICAL RESULTS

5.1. Steady case

In order to assess the stability and the quality of the finite element formulation described above, the problem (35)–(36) is studied in a cubic domain ($0 \le x \le 1$, $0 \le y \le 1$, $0 \le z \le 1$). The velocity vector is fixed to $\mathbf{U} = (1, 0, 0)^T$. The Dirichlet boundary conditions and the sollicitation vector $\mathbf{f} = (2x - 2\eta, -2\eta, 2z)^T$ are imposed in such a way as to reproduce approximately an arbitrary solution of the continuous problem, namely $\mathbf{B} = (x^2, y^2, -2(x+y)z)^T$ and $p = 0$. The dissipation coefficient τ_1 can be given by one or the other of the two following expressions:

$$\tau_1 = \alpha \frac{h^2}{4\eta}, \tag{37}$$

$$\tau_1 = \alpha \left(\left(\frac{2\|\mathbf{U}\|}{h} \right)^2 + \left(\frac{4\eta}{h^2} \right)^2 \right)^{-1/2}. \tag{38}$$

The penalization factor τ_2 could be set to either $\tau_2 = 0$, which corresponds to the original physical model, or to $\tau_2 = \|\mathbf{U}\|h/2$. In the later case the coefficient $r = \tau_2 - \eta$ ends up to be:

$$r = \eta \left(1 - \frac{Re_{\mathrm{m}_h}}{2} \right), \tag{39}$$

where Re_{m_h} is the local magnetic Reynolds number defined by:

$$Re_{\mathrm{m}_h} = \sigma\mu \|\mathbf{U}\| h. \tag{40}$$

Computations have been made for two different magnetic diffusion coefficients $\eta = 1.2 \times 10^{-1}$ and $\eta = 1.2 \times 10^{-3}$ representing respectively, a highly diffusive case and a highly convective one, and for $\alpha = 0.1$, $1/3$ and 1.0. For each case, the mesh variation of the $\mathbf{L}_2(\Omega)$-norms of the magnetic divergence $\|\nabla \cdot \mathbf{B}_h\|$, the error $\|\mathbf{B}_h - \mathbf{B}\|$, the Lagrange multiplier $\|p_h\|$ and its gradient $\|\nabla p_h\|$ were all calculated.

Comments:

Highly convective case

If the magnetic convection is important ($\eta = 1.2 \times 10^{-3}$), the best solutions are obtained with $\tau_2 = \|\mathbf{U}\|h/2$ and this is true quite independently of the expression used for τ_1. Actually, the methods generated with $\tau_2 = \|\mathbf{U}\|h/2$ are much more conservative and accurate than the 'Helmholtz' formulation and the approximation obtained with $\tau_2 = 0$ (Figure 1(a) and (b)).

However it should be noticed that the expression for τ_1 given in (38), which in this case is of order $O(h)$ in the convective-dominant case, gives rise to optimal convergence rates for both $\mathbf{B}_h$ and p_h. In fact, for the Lagrange multiplier p error and the magnetic field error, the convergence rate is 2. For the gradient of p_h and the divergence of $\mathbf{B}_h$, the rates are around unity (Figure 2).

When τ_1 is fixed to its expression in Equation (37), which in the convective-dominant case is of order $O(h^2)$, the convergence rates are still optimal for the magnetic induction field and for its divergence, while for p and its gradient the rates become suboptimal. For p_h, the rate is around 1 and the gradient of p_h seems to be bounded by a constant. Figure 3 shows these convergence rates for $\alpha = 0.1$.

When compared together, the method generated by Equation (38) gives rise to better accuracy and magnetic conservation than the method generated by Equation (37). The methods do not seem to be very sensitive to the value of the constant α, so $\alpha = 0.1$, seems a suitable value to be assigned.

If $\tau_2 = 0$ and the convection is still dominant, then the accuracy of the method is very poor and the error norms are very important, especially when Equation (37) is used for τ_1. Regardless of the expression τ_1 used, the method is very sensitive to the value of the constant α showing signs of instabilities due to the effect of the convection. No general trend for the convergence rates could be drawn. Thus, one should avoid using such a method.

Highly diffusive case

When diffusion is dominant ($\eta = 1.2 \times 10^{-1}$), all the methods obtained by the different expressions of τ_1 and τ_2 are accurate, convergent and stable. When $\tau_2 = 0$, both expressions

(37) and (38) for τ_1 give rise to approximately the same results in terms of error and magnetic divergence. This could be explained by the fact that since the magnetic diffusion is dominant, Equations (37) and (38) lead both to expressions of $O(h_2)$.

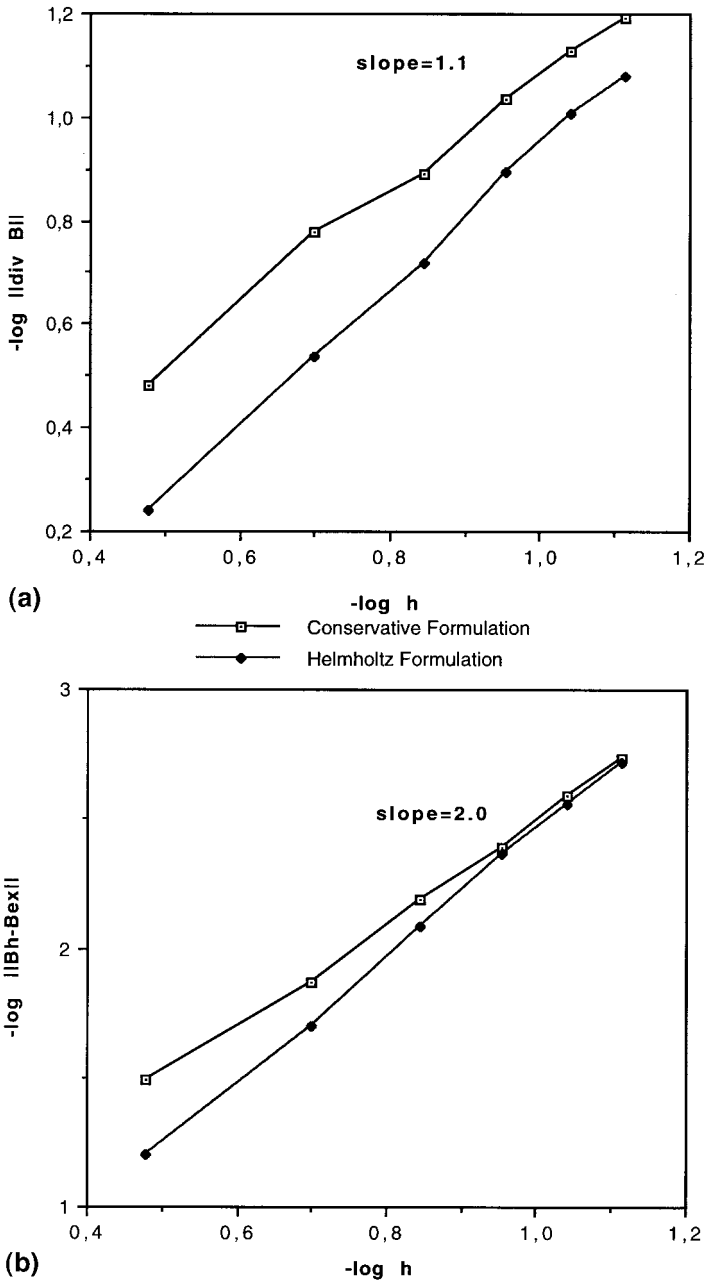

Figure 1. (a) The L_2 norms of the magnetic field divergence vs. the mesh size. Comparison between the Helmholtz formulation and conservative formulation with: $\tau_1 = 0.1((2\|U\|/h)^2 + (4\eta/h^2)^2)^{-0.5}$; $\tau_2 = \|U\|h/2$; $\eta = 1.2 \times 10^{-3}$. (b) The L_2 norms of the magnetic field divergence vs. the mesh size. Comparison between the Helmholtz formulation and conservative formulation with: $\tau_1 = 0.1((2\|U\|/h)^2 + (4\eta/h^2)^2)^{-0.5}$; $\tau_2 = \|U\|h/2$; $\eta = 1.2 \times 10^{-3}$.

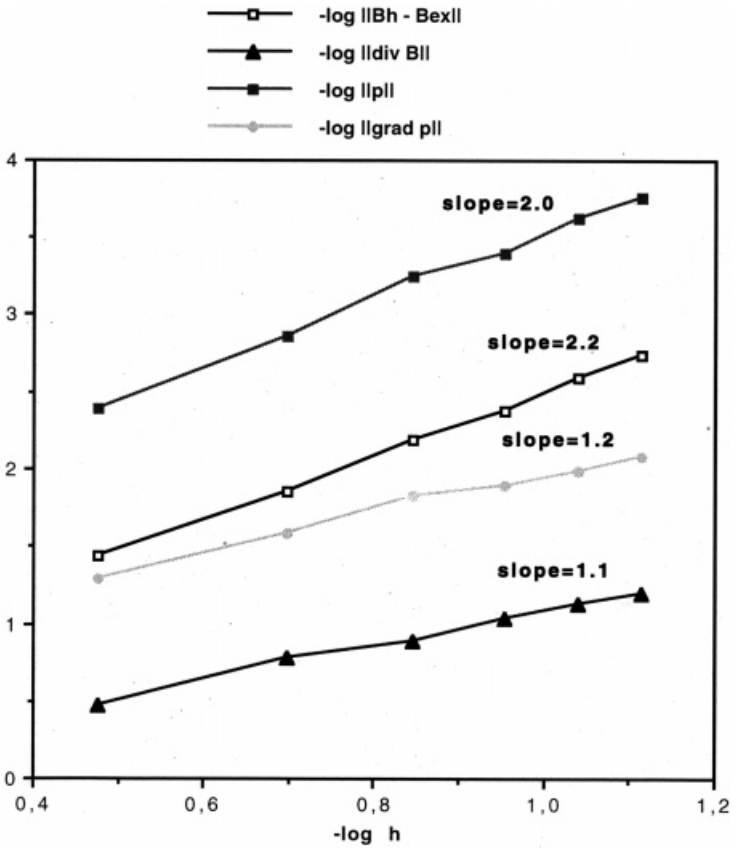

Figure 2. Different L_2 norms vs. the mesh size; conservative formulation with $\tau_1 = 1.0((2\|U\|/h)^2 + (4\eta/h^2)^2)^{-0.5}$; $\tau_2 = \|U\|h/2$; $\eta = 1.2 \times 10^{-3}$.

The convergence rates, obtained for the two expressions of τ_1 are the same. Convergence rates of 1 were obtained for the magnetic field divergence and for the scalar p. The convergence rate for the magnetic induction is of order 2 and the gradient of p is bounded by a constant (Figure 4). As expected, the linear interpolation on tetrahedral elements keeps the optimal convergence rates for the magnetic induction and its gradient, while p and its gradient convergence at suboptimal rates.

When $\tau_2 = \|\mathbf{U}\|h/2$, the best results were obtained in terms of the error on $\mathbf{B}_h$ and on its divergence. However, the differences between these results and those obtained with $\tau_2 = 0$ are not very important. Again the convergence rates are those expected, optimal for the magnetic field and suboptimal for the scalar p (Figure 5). Once more, the results obtained are quite independent of τ_1 and of the constant α.

5.2. Unsteady case

In order to highlight the advantages of using the conservative stable formulation (35)–(36) rather than a formulation derived from the 'Helmholtz' equation (11), one should look at the behavior of the solutions obtained with the two methods, for an unsteady problem, and compare them in terms of the norm of the divergence of the magnetic field. In the same

manner as in Section 5.1, the velocity vector $\mathbf{U} = (1, 0, 0)^T$, the sollicitation force vector $\mathbf{f} = (2x - 2\eta + 1, -2\eta, 2z)^T$ and the Dirichlet boundary conditions are imposed in such a way as to reproduce approximately an arbitrary unsteady solution of the continuous problem $\mathbf{B} = (x^2 + t, y^2, -2(x + y)z)^T$ and $p = 0$. Computations have been made with the following coefficients: $\tau_1 = 1.0h^2/4\eta$, $\tau_2 = \|\mathbf{U}\|h/2$ and $\eta = 1.2 \times 10^{-1}$.

Figures 6 and 7 show the evolution of the divergence of the magnetic field as a function of the time steps. In Figure 6, the first 50 time steps are highlighted, while in Figure 7 the number of time steps is set to 1000. It is seen that the conservative formulation performs much better than the 'Helmholtz' formulation. It reaches an 'optimal' value after a few time steps, then it almost keeps on that same divergence (in reality the norm of the divergence keeps on reducing). With the 'Helmholtz' formulation, the divergence first increases then is reduced to a constant plateau that is approximately five times higher than the one obtained with the conservative formulation.

5.3. The Hartmann–Poiseuille flow

The Hartmann flow is one of the cornerstone examples of the MHD flows (Moreau [23]). The validation of any MHD code should use this flow as a benchmark test. Suppose a liquid metal flowing under the influence of a pressure gradient, in the x-direction, through a

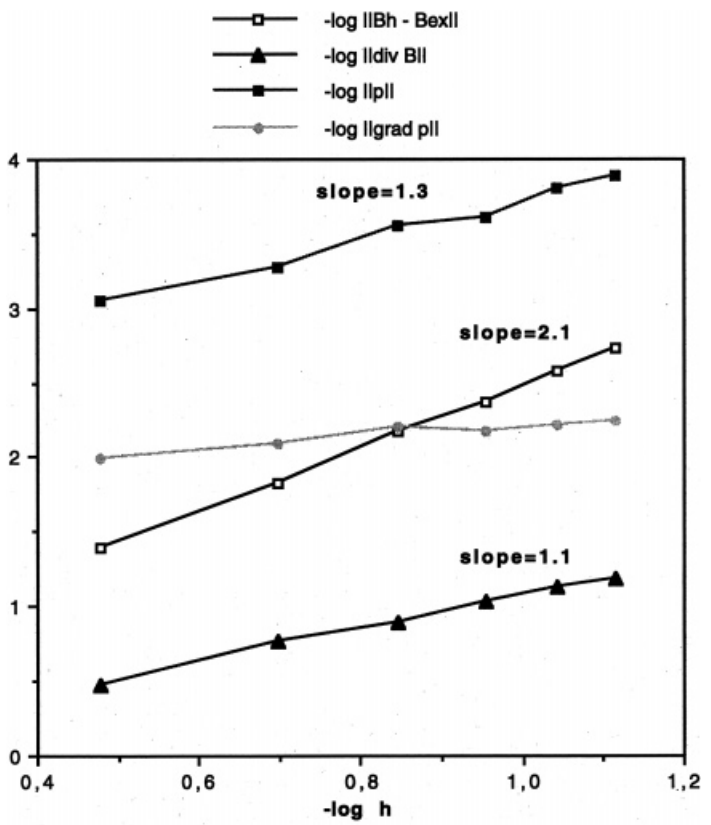

Figure 3. Different L_2 norms vs. the mesh size; conservative formulation with $\tau_1 = 0.1(h^2/4\eta)$; $\tau_2 = \|U\|h/2$; $\eta = 1.2 \times 10^{-3}$.

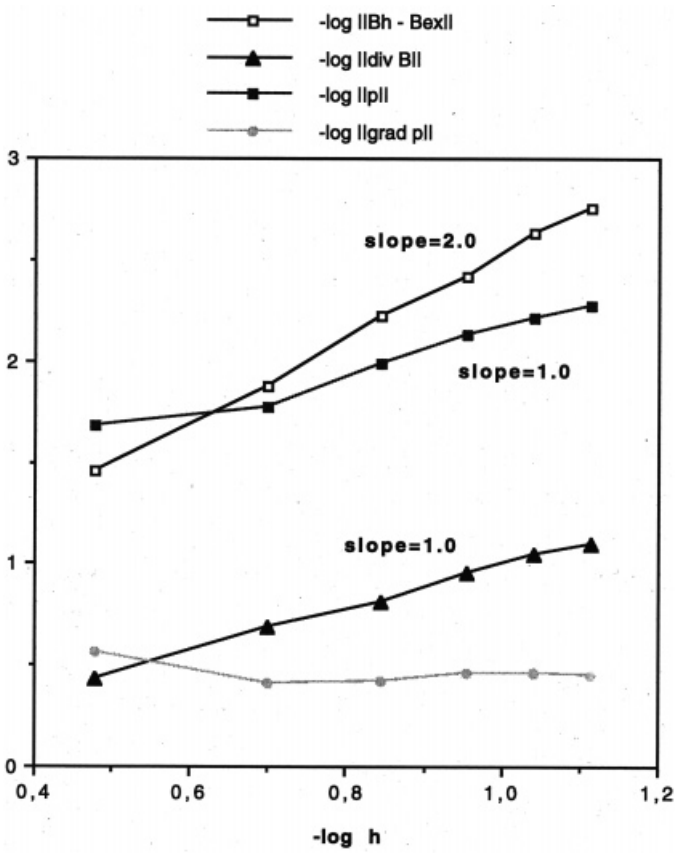

Figure 4. Different L_2 norms vs. the mesh size; conservative formulation with $\tau_1 = 0.1(h^2/4\eta)$; $\tau_2 = 0$; $\eta = 1.2 \times 10^{-1}$.

rectangular cross-section duct that is infinitely long in the z-direction. Suppose a uniform external magnetic field $\mathbf{B}_0$ is applied along the y-direction. The liquid flow induces a perturbation of the imposed magnetic field $\mathbf{B}_0$, that is in the same x-direction as the flow. Assuming that the walls are at $y = \pm L$ and are perfectly insulating, using the non-slip boundary conditions for the velocity and assuming the perturbation of the magnetic field to be zero at these walls, the problem has an analytical solution for the velocity and the magnetic field, that can be put in the following form:

$$\mathbf{U}_x = -\frac{\rho G Ha}{gs\mathbf{B}_0^2}\left(\frac{\cosh(Ha) - \cosh(yHa/L)}{\sinh Ha}\right), \tag{41}$$

$$\mathbf{B}_x = -\frac{\mathbf{B}_0 Re_{\mathrm{m}}}{Ha}\left(\frac{\sinh(yHa/L) - (y/L)\sinh(Ha)}{\cosh(Ha) - 1}\right), \tag{42}$$

where $\mathbf{B}_x$ and $\mathbf{U}_x$ are respectively, the x-components of the magnetic and the velocity fields, ρG the pressure gradient keeping the fluid in motion (ρ being the density) and Re_{m} and Ha are the magnetic Reynolds number and the Hartmann number respectively, defined as:

$$Re_{\mathrm{m}} = \sigma\mu UL, \tag{43}$$

$$Ha = \mathbf{B}_0 L\left(\frac{\sigma}{\rho v}\right)^{1/2}. \tag{44}$$

The square of the Hartmann number is the ratio between the electromagnetic forces and the viscous forces. In Equation (43), U is the velocity $\mathbf{U}_x$ at $y = 0$ and v is the kinematic viscosity of the liquid metal.

The Hartmann flow with the velocity field given as an input data, has been computed for the following physical parameters: $\sigma = 7.14 \times 10^5$ $(\Omega\,\mathrm{m})^{-1}$, $\eta = 1.2 \times 10^{-1}$ $\mathrm{m^2\,s^{-1}}$, $\rho v = 1.5 \times 10^{-4}$ $\mathrm{kg\,m^{-1}\,s^{-1}}$, $\rho G = 4.85 \times 10^{-5}$ $\mathrm{Pa\,m^{-1}}$, $L = 0.5$ m, $\mathbf{B}_0 = 1.4494 \times 10^{-4}$ Tesla. The results obtained from the analytical solution are compared with the results from the numerical computations. The agreement between the two is quite good (Figure 8). Then a parametric study is made using the Hartmann number as a parameter ($Ha = 1$, 2, 5, 10, 20) (Figure 9). This parametric study shows a very good agreement with the analytical solution. Furthermore, this study puts into evidence the building of the Hartmann layer.

Figure 10 shows the analytical solution for the velocity ($Ha = 1$, 2, 5, 10, 20). It is seen that the intensity of the applied transversal magnetic field influences the velocity field. From a Poiseuille profile when the magnetic field is zero ($Ha = 0$), the velocity is flattened and becomes quite constant in the core region of the duct, with the gradient of the velocity concentrated in two boundary layers (Hartmann layer) near the walls, when the magnetic field is strong ($Ha \gg 1$). The flattening of the velocity profile is due to the magnetic braking of the flow. In

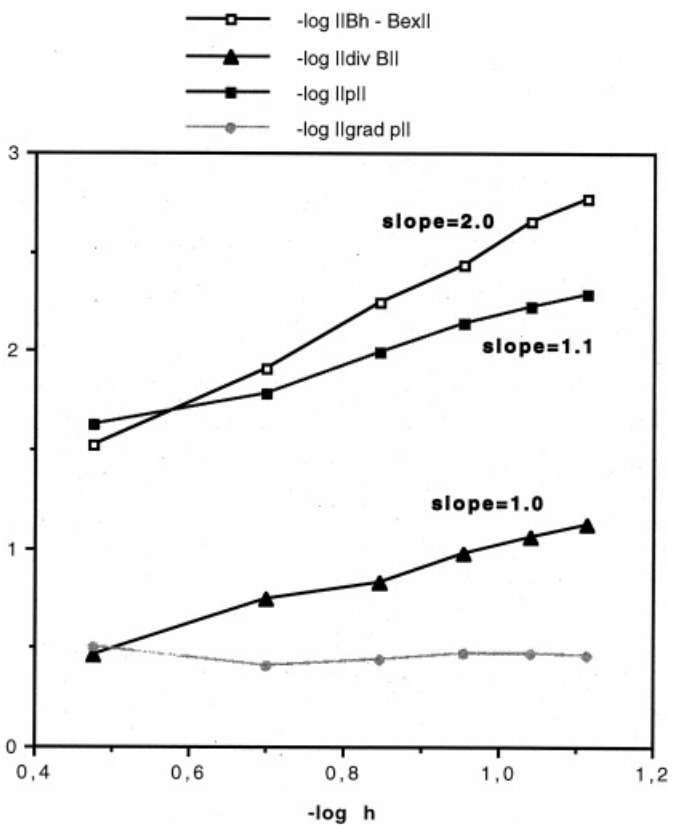

Figure 5. Different L_2 norms vs. the mesh size; conservative formulation with $\tau_1 = 0.1(h^2/4\eta)$; $\tau_2 = \|U\|h/2$; $\eta = 1.2 \times 10^{-1}$.

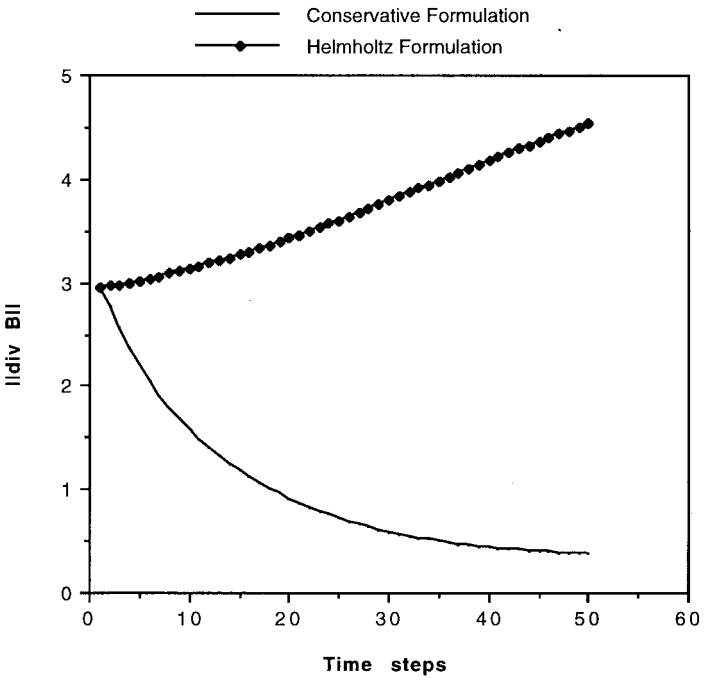

Figure 6. The L_2 norms of the magnetic field divergence vs. the time steps number. Comparison between the Helmholtz formulation and the conservative formulation with: $\tau_1 = 0.1(h^2/4\eta)$; $\tau_2 = \|U\|h/2$; $\eta = 1.2 \times 10^{-1}$.

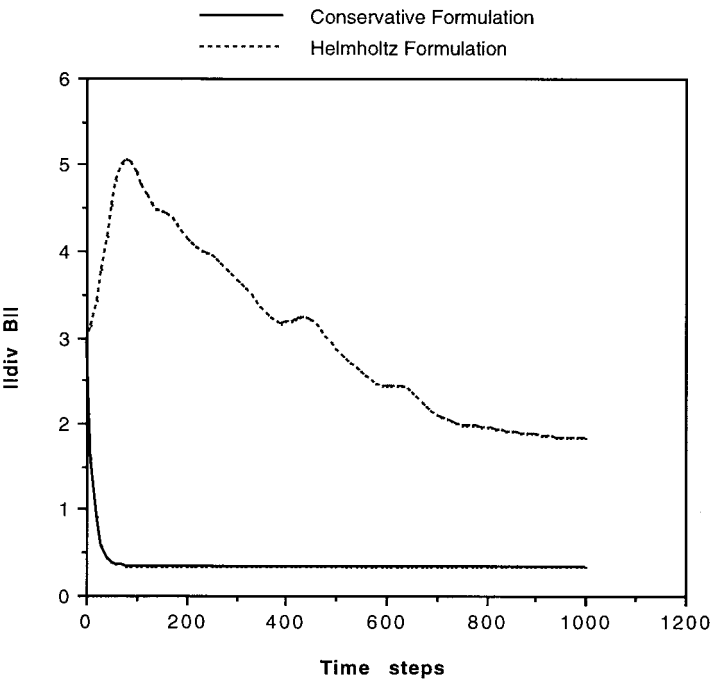

Figure 7. The L_2 norms of the magnetic field divergence vs. the time steps number. Comparison between the Helmholtz formulation and the conservative formulation with: $\tau_1 = 0.1(h^2/4\eta)$; $\tau_2 = \|U\|h/2$; $\eta = 1.2 \times 10^{-1}$.

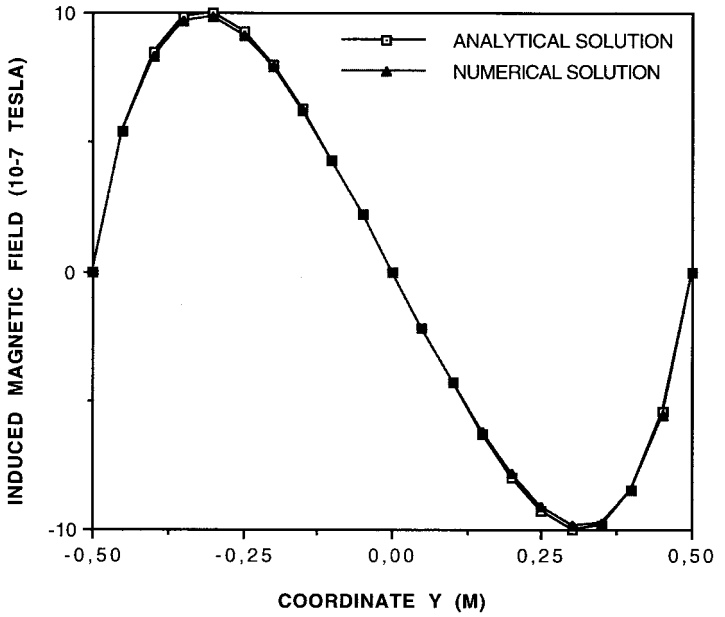

Figure 8. The induced magnetic field along the y-axis; $Ha = 3.45$, $Re_m = 0.0916$.

Figure 9, one can see the magnetic signature of this boundary layer and as the Hartmann number is increased from 1 to 20, one can see a boundary layer type behavior developing for the induced magnetic field (Figure 9).

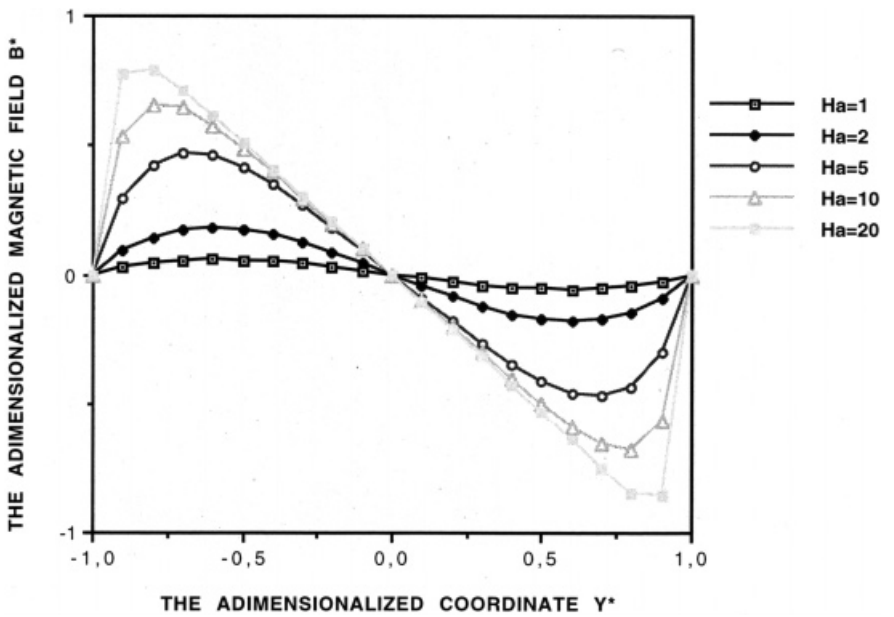

Figure 9. The induced adimensionalized magnetic field **B*** along the adimensionalized co-ordinate **Y*** ($\mathbf{B}^* = B_x B_0 / \mu\rho GL$, $Y^* = y/L$).

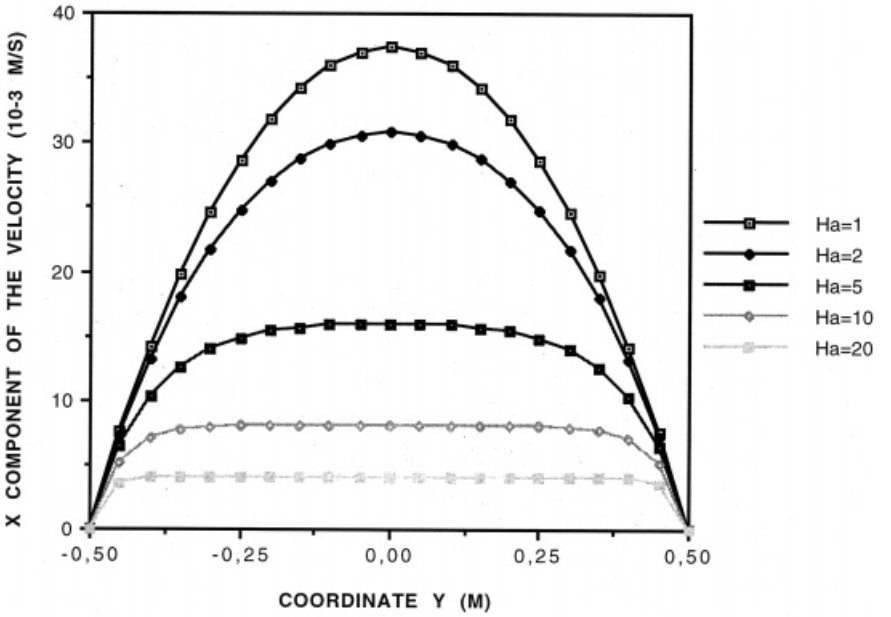

Figure 10. The x-component of the velocity along the y-axis.

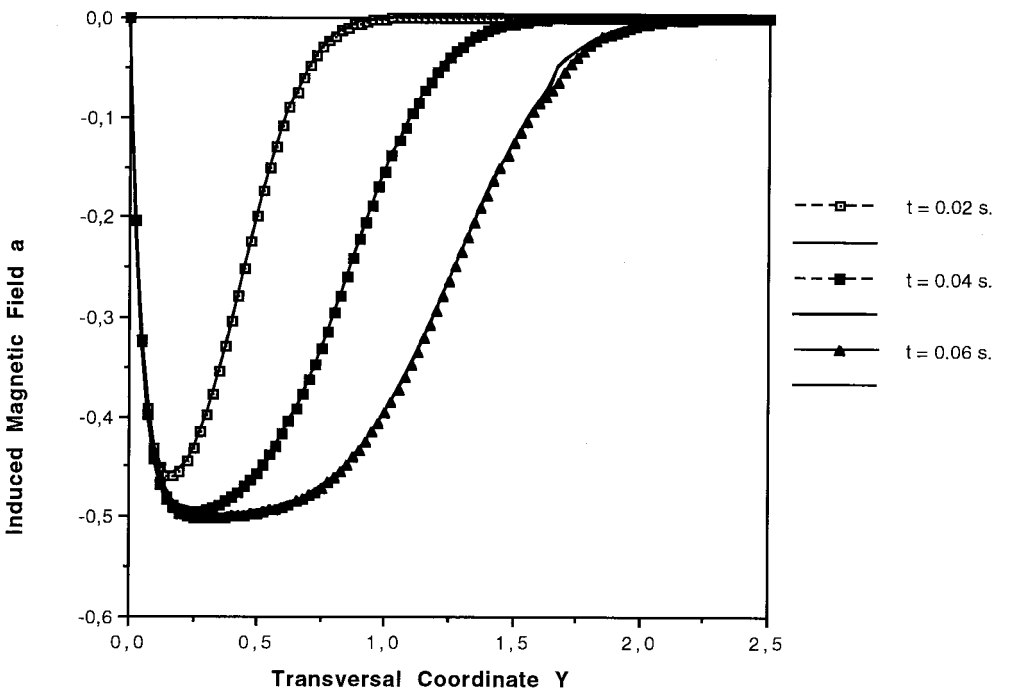

Figure 11. The evolution of the induced magnetic field a vs. the co-ordinate y for different times t; comparison between analytical and numerical solutions.

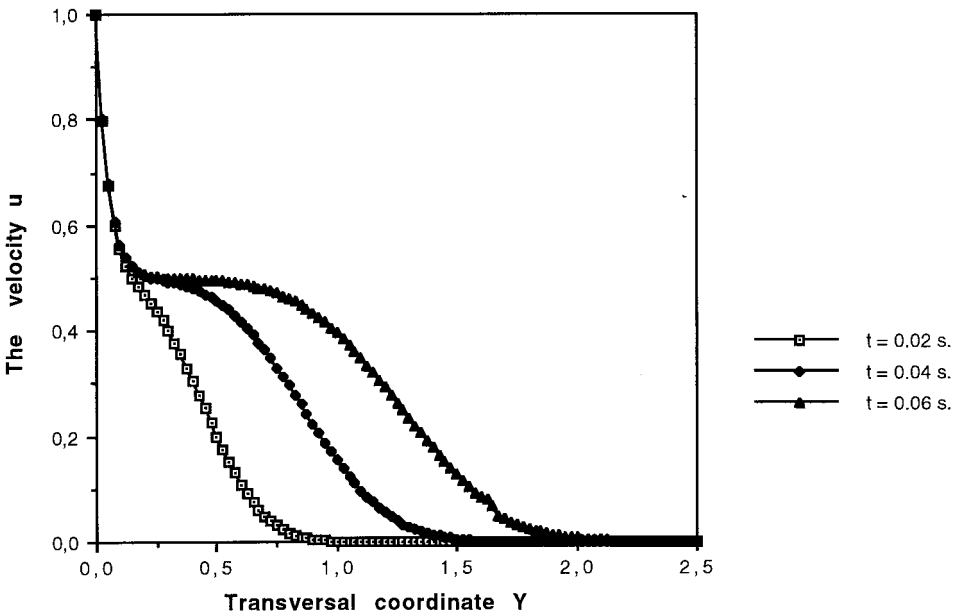

Figure 12. The evolution of the velocity u vs. the co-ordinate y for different times t; the analytical solution.

This behavior can be put into evidence because the walls are perfectly insulating, which allows the use of the Dirichlet conditions for the magnetic field. If the walls were perfectly conducting then the boundary conditions should be set to the Neumann-type conditions and hence the magnetic signature of the Hartmann layer would disappear.

5.4. The MHD Rayleigh flow

Suppose an infinite plane plate is at rest in a semi-infinite domain that is electrically conducting. Let $\mathbf{B}_0 = 0$ be an applied magnetic field along y, the co-ordinate normal to the plate. Suppose the plate is suddenly set in motion at $t = 0$, with a constant velocity U. Then, the motion propagates within the fluid domain as a wave. Ahead of this diffusive wave front, the fluid is still at rest; before the front, the fluid is in motion. Within the moving fluid, one can distinguish two regions: The Hartmann layer in the vicinity of the plane plate, which has a characteristic thickness $\delta = (\rho\nu/\sigma)^{1/2}/\mathbf{B}_0$, and a second region that is essentially a uniform plateau where the velocity is maximum and constant. The development of such a velocity field induces a perturbation in the imposed magnetic field. This perturbation travels as a plane wave. This wave is called the Alfven wave and travels within the fluid domain with a constant velocity $A_0 = \mathbf{B}_0/(\mu\rho)^{1/2}$. When the kinematic viscosity of the fluid is equal to its magnetic diffusivity, then the magnetic Prandlt number is equal to one ($Pr_m = \nu/\eta$), and an analytical solution exists for the MHD Rayleigh problem (Moreau [23]).

This analytical solution could be written in the following form:

$$u = \frac{U}{4}\left(2 - (\mathrm{erf}\lambda_+ + \mathrm{erf}\lambda_-) + \mathrm{e}^{-A_0 y/d}(1 - \mathrm{erf}\lambda_-) + \mathrm{e}^{A_0 y/d}(1 - \mathrm{erf}\lambda_+)\right), \tag{45}$$

$$a = \frac{U}{4}\left((\mathrm{erf}\lambda_- - \mathrm{erf}\lambda_+) + \mathrm{e}^{-A_0 y/d}(1 - \mathrm{erf}\lambda_-) - \mathrm{e}^{A_0 y/d}(1 - \mathrm{erf}\lambda_+)\right), \tag{46}$$

where

$$\lambda_{\pm} = \frac{y \pm A_0 t}{2(dt)^{1/2}}, \tag{47}$$

$$d = \nu = \eta, \tag{48}$$

$$a = \frac{b}{(\mu\rho)^{1/2}}, \tag{49}$$

and u and b are the x-components of the velocity field and the induced magnetic field respectively. This MHD Rayleigh problem, with the velocity space field given as an input data, has been computed with the following physical parameters: $\sigma = (10^7/(4\pi))\ (\Omega\,\mathrm{m})^{-1}$, $\eta = 1.0\ \mathrm{m^2\,s^{-1}}$, $\rho = 0.4 \times 10^{-4}\ \mathrm{kg\,m^{-1}\,s^{-1}}$, $\mathbf{B}_0 = 1.4494 \times 10^{-4}$ Tesla and for $t \leq 0.08$ s. The results obtained from the analytical solution and the numerical computations are compared. The agreement between the two is quite perfect (Figure 11). The three regions (Hartmann layer, the magnetic plateau and the wave front) are clearly distinguished. Figure 12 shows the corresponding analytical solution of the velocity field $u(y, t)$.

6. CONCLUSIONS

A stabilized conservative finite element method for the 3D MHD equations is proposed. It is seen that the stability and the convergence of the method depends on the expressions of the coefficients τ_1 and τ_2. The method has been validated through steady and unsteady tests. The method was then used for computing the Hartmann flow through a duct and the MHD Rayleigh flow around a moving plane plate. The results are seen to be in a very good agreement with the analytical solutions.

For industrial scale problems, the convection of the magnetic field is negligible when compared with its diffusion. Hence, if $\tau_2 = 0$ and $\tau_1 = h^2/4\eta$, one obtains a method that is stable, accurate and quite simple. Moreover, since the conservation law is solved within the system, this method is more conservative regarding the norm of the magnetic field divergence than the 'Helmholtz' formulation.

At astrophysical scales when convection is much more important than diffusion, $\tau_2 = \|\mathbf{U}\|h/2$ and $\tau_1 = ((2\|\mathbf{U}\|/h)^2 + (4\eta/h^2)^2)^{-1/2}$ are more appropriate expressions to be used in order to generate a stable and convergent formulation. Furthermore, these parameters generate methods that are more conservative than the 'Helmholtz' formulation, and the difference between the divergence norms calculated for the two methods are quite important.

When the MHD phenomenon to be studied is an unsteady one, then the advantages of using the conservative method with the appropriate coefficients are obvious. While the conservative method keeps on reducing the divergence of the vector solution, the 'Helmholtz' formulation gives rise to solutions that are much less accurate.

REFERENCES

1. M. Gyimesi and J.D. Lavers J.D., 'Generalized potential formulations for magnetostatic problems', *IEEE Trans. Magn.*, **28**, 1924–1929 (1992).
2. O.C. Zienkiewicz, J. Lyness and D.R.J. Owen, 'Three-dimensional magnetic field determination using a scalar potential, a finite element solution', *IEEE Trans. Magn.*, **13**, 1649–1656 (1977).
3. V. K. Garg and J. Weiss, 'Finite element solution of transient eddy current problems in multiply exited magnetic systems', *IEEE Trans. Magn.*, **22**, 1257–1259 (1986).

4. S.C. Tandon and V.K. Chari, 'Transient solution of the diffusion equation by the finite element method', *J. Appl. Phys.*, **52**, 2431–2432 (1981).
5. O. Biro and K. Preis, 'On the use of magnetic vector potential in the finite element analysis of three-dimensional eddy currents', *IEEE Trans. Magn.*, **25**, 3145–3159 (1989).
6. Y.R. Fautrelle, 'Analytical and numerical aspects of electromagnetic stirring induced by alternating magnetic fields', *J. Fluid Mech.*, **102**, 405–430 (1981).
7. A.J. Mestel, 'Magnetic levitation of liquid metals', *J. Fluid Mechs.*, **117**, 27–43 (1982).
8. S.D. Lympany, J.W. Evans and R. Moreau, 'Magneto-hydrodynamic effects in aluminium reduction cells; metallurgical applications of magneto-hydrodynamics, in H.K. Moffat and M.R.E. Proctor (eds.), *Proc. Symp. Int. Union of The Theoritical and Applied Mechanics*, Cambridge, UK (September 6–10, 1982), The Metals Society, London, 1984, pp. 15–23.
9. O. Besson, J. Bourgeois, P.A. Chevalier, J. Rappaz and R. Touzani, 'Numerical modelling of electromagnetic casting processes', *J. Comp. Phys.*, 92, 482–507 (1991).
10. H.J. Conraths, 'Eddy current and temperature simulation in thin moving metal strips', *Int. J. Numer. Methods Eng.*, **39**, 141–163 (1996).
11. S.S. Sazhin, M. Makhlouf and T. Ishii, 'Solutions of magneto-hydrodynamic problems based on a conventional computational fluid dynamics code', *Int. J. Numer. Methods Fluids*, **21**, 433–442 (1995).
12. L.T.R. Gardner and G.A. Gardner, 'A two-dimensional bicubic and B-spline finite element: used in a study of MHD duct flow', *Comp. Methods Appl. Mech. Eng.*, **124**, 365–375 (1995).
13. T. Tanahashi and Y. Oki, 'Numerical analysis of natural convection of thermo-electrically conducting fluids in a square cavity under a uniform magnetic field', *JSME Int. J.*, **38**, 374–381 (1995).
14. T. Tanahashi and Y. Oki, 'Numerical analysis of natural convection of thermo-electrically conducting fluids in a square cavity under a uniform magnetic field (calculated results, frequency characteristics)', *JSME Int. J.*, **39**, 508–516 (1996).
15. N. Ben Salah, A. Soulaïmani, W.G. Habashi and M. Fortin, 'A conservative stabilized finite element method for the magneto-hydrodynamic equations, in S.N. Atluri and G. Yagawa (eds.), *Advances in Computational Engineering Science*, *International Computational Engineering and Science 97*, Tech Science Press, Forsyth, GA, 1997, pp. 269–276.
16. L.D. Landau, E.M. Lifshitz and L.P. Pitaevskii, *Electrodynamics of Continuous Media*, Pergamon, Oxford, 1984.
17. B. Jiang, J. Wu and L.A. Povinelli, 'The origin of spurious solutions in computational electromagnetics', *NASA-TM-106921*, *E-9633*, *ICOMP-95-8*, 1995.
18. H. Brezis, *Analyse Fonctionnelle*, *Theorie et Applications; Collection Mathématiques Appliquées pour la Maîtrise sous la Direction de P.G. Ciarlet et J.L. Lions*, Masson, Paris, 1983.
19. F. Brezzi and M. Fortin, *Mixed and Hybrid Finite Element Methods*, Springer Series in Computational Mathematics vol. 15, Springer, Berlin, 1991.
20. T. Hugues, L. Franca and M. Ballestra, 'A new finite element formulation for computational fluid dynamics: V. Circumventing the Babuska–Brezzi condition: a stable Petrov–Galerkin formulation of the Stokes problem accommodating equal-order interpolations', *Comp. Methods Appl. Mech. Eng.*, **59**, 85–99 (1986).
21. F. Brezzi and J. Pitkaranta, 'On the stabilization of finite element approximations of the Stokes problem', in W. Hackbusch (ed.), *Efficient Solutions of Elliptic Systems*, *Vieweg Notes on Numerical Fluid Mechanics*, vol. 10, Vieweg, Wiesbaden, 1984, pp. 11–19.
22. G.S. Baruzzi, W.G. Habashi and M.M. Hafez, 'A second-order finite element method for the solution of the transonic Euler and Navier–Stokes equations', *Int. J. Numer. Methods Fluids*, **20**, 671–693 (1995).
23. R. Moreau, *Magneto-hydrodynamics*, Kluwer, Dordrecht, 1990.

